

Self-organized critical forest-fire model on large scales

Klaus Schenk,¹ Barbara Drossel,^{2,*} and Franz Schwabl¹

¹*Physik-Department der Technischen Universität München, James Franck Straße, D-85747 Garching, Germany*

²*Physics Department, Raymond and Beverley Sackler Faculty of Exact Sciences, Tel Aviv University, Tel Aviv 69978, Israel*

(Received 7 May 2001; published 23 January 2002)

We discuss the scaling behavior of the self-organized critical forest-fire model on large length scales. As indicated in earlier publications, the forest-fire model does not show conventional critical scaling, but has two qualitatively different types of fires that superimpose to give the effective exponents typically measured in simulations. We show that this explains not only why the exponent characterizing the fire-size distribution changes with increasing correlation length, but allows us also to predict its asymptotic value. We support our arguments by computer simulations of a coarse-grained model, by scaling arguments and by analyzing states that are created artificially by superimposing the two types of fires.

DOI: 10.1103/PhysRevE.65.026135

PACS number(s): 05.65.+b, 05.45.Df, 05.70.Jk, 05.70.Ln

I. INTRODUCTION

During the past years, systems that exhibit self-organized criticality (SOC) have attracted much attention, since they might explain part of the abundance of fractal structures in nature [1]. Their common features are slow driving or energy input and rare dissipation events that are instantaneous on the time scale of driving. In the stationary state, the size distribution of dissipation events obeys a power law, irrespective of initial conditions and without the need to fine tune parameters. Examples of such systems are the sandpile model [1], the self-organized critical forest-fire model (FFM) [2–5], the earthquake model by Olami, Feder, and Christensen [6], and the Bak-Sneppen model [7,8]. A recent review on the literature on SOC can be found, for instance, in [9].

The study of SOC models is usually based on the assumption that the size distribution $n(s)$ of dissipation events (avalanches, fires, earthquakes) shows the scaling behavior familiar from equilibrium critical systems,

$$n(s) \approx s^{-\tau} \mathcal{C}(s/s_{\max}), \quad (1)$$

with a cutoff function \mathcal{C} that is constant for small arguments and decays exponentially fast when the argument is considerably larger than 1. The cutoff cluster size s_{\max} is related to the correlation length ξ via $s_{\max} \sim \xi^D$, with D being the fractal dimension of the dissipation events. (If the cutoff is set by the system size L , ξ must be replaced with L .) This holds indeed for some self organized critical systems, like the Bak-Sneppen model, but it has been known for some time that it does not hold for the two-dimensional Abelian sandpile model [10]. Very recent work has shown that this violation of simple scaling in the sandpile model is due to the existence of multiple waves of topplings, and some features of the correct scaling behavior have been worked out [11,12]. Violation of finite-size scaling is also seen in the above-mentioned earthquake model [13].

During recent years, evidence has accumulated that the two-dimensional SOC forest-fire model does not show simple scaling either. Instead, there are more than one diverging length scale [14], the behavior of the model for tree densities just above the critical density is completely different from that of conventional critical systems [15,16], and finite-size scaling is violated [17]. A scaling collapse based on Eq. (1) gives a good overlap of the tails of the distribution, but not so much of the first part, where the slope (i.e., the exponent τ) seems to increase slightly with increasing correlation length (see, e.g., [4], and Fig. 2 below). We have suggested [17] that all these features are due to the fact that there are two qualitatively different types of fires in the system: smaller, fractal fires that occur in regions of low tree density and burn a tree cluster that resembles a percolation cluster, and larger compact fires that burn a patch of a tree density above the percolation threshold.

The purpose of this paper is to show how these two types of fires add up to give the distributions typically seen in computer simulations, and to derive the asymptotic properties of the fire size distribution in the limit of very large correlation length. In particular, we will derive the asymptotic value of the exponent of the fire size distribution, toward which it should converge for sufficiently large correlation length. We support our arguments by three different types of evidence that all lead to the same conclusions: (i) Scaling arguments based on the superposition of the mentioned two types of fires; (ii) The fire size distributions resulting from the (artificial) superposition of the fires of patches of different tree densities and different sizes; (iii) Computer simulations of a coarse-grained model that allow us to numerically study systems with much larger correlation length than has been possible so far. The outline of the paper is as follows: In the next section, we will derive scaling laws and analytical expressions for the fire size distribution resulting from the assumption that the forest-fire model is composed of patches of different sizes and different tree densities. Then, in Sec. III we will show numerical data that result from the superposition of fires from artificially generated patches of different sizes and densities. In Sec. IV, we will present and study a coarse-grained forest-fire model where

*Present address: Technischen Universität München, James Franck Strasse, D-85747 Garching, Germany

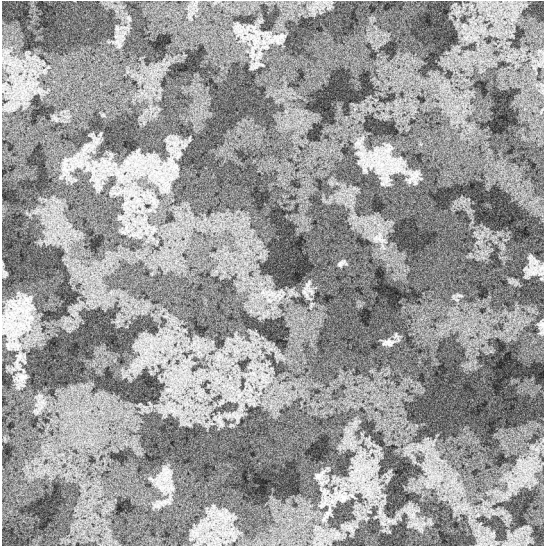


FIG. 1. Snapshot of the SOC forest-fire model for $\rho \approx \rho_c \approx 0.408$ and system size $L = 4096$. Trees are black and empty sites are white.

each lattice site stands for a group of several sites in the original model. Finally, we will discuss our findings.

II. SCALING PROPERTIES OF THE SOC FOREST-FIRE MODEL

A. The definition of the model

The SOC forest-fire model is usually studied on a square lattice with L^2 sites. Each site is either occupied by a tree, or is empty. At each time step, all sites are updated in parallel according to the following rules: (i) An empty site becomes occupied by a tree with probability p , (ii) A tree is struck by lightning with probability f . This tree and the whole cluster of trees connected to it (by nearest-neighbor coupling) burn down and become empty sites.

B. Two types of fires determine the dynamics of the SOC forest fire model

As long as p and f are so small that fires do not interfere with each other or with tree growth, the stationary behavior of the model depends only on the ratio f/p , but not on the two parameters separately. After some time, the system reaches a stationary state with a mean tree density ρ and a mean fire size \bar{s} . A snapshot of the two-dimensional (2D) system in the stationary state is shown in Fig. 1. One can see that it consists of patches of different tree densities and different sizes. Some of the patches have a high tree density, and if they are struck by lightning, the entire patch burns down, with only few trees being left. After the fire, the tree density $\rho_{\text{patch}}(t)$ of the patch grows again according to

$$\dot{\rho}_{\text{patch}}(t) = p(1 - \rho_{\text{patch}}(t)) \quad (2)$$

until it is hit by the next lightning stroke. This mechanism of

growth and burning down of forest clusters produces the patchy structure seen in Fig. 1, which is characterized by the following properties.

(a) The patches are almost homogeneously covered with trees. This is because a fire that burns a patch usually leaves only a few trees behind. (We found that the local tree density within a patch immediately after a fire is typically 0.078 for the 2D square lattice and 0.062 for the 2D triangular lattice). Thus the random tree growth leads to a uniform tree density within the patch. The size distribution of tree clusters within a patch is therefore similar to the size distribution of clusters in a percolation system of the same density. (By ‘‘percolation’’ we mean ‘‘uncorrelated percolation’’ throughout this paper. For an introduction to percolation theory, see [18].) The fact that several patches contain larger dense tree clusters indicates that some fires leave behind small clusters that can become seeds of new patches. This process of birth and death of patches, which happens on a slower time scale, does not affect our main argument.

(b) It can be assumed that the distribution of patch sizes is independent of their tree density, because a fire in most cases hardly changes the size of a patch. Thus, the size of most patches is the same for high and low tree density.

(c) Some patches have a tree density above the percolation threshold. These patches contain a spanning cluster that is compact, i.e., has the fractal dimension 2. When such a patch is struck by lightning, a compact fire occurs that burns the spanning cluster. If lightning strikes a patch of low tree density (below the percolation threshold), only a small, fractal cluster of trees burns down, and only part of the patch is affected by the fire. If the mean fire size is large (i.e., if f/p is small), most trees burn down during large fires, and most of the empty sites are created during the large compact fires, resulting in the above-mentioned low local tree density immediately after a fire.

(d) The size of the largest patch diverges for $f/p \rightarrow 0$, suggesting that the system is close to a critical point and can be characterized by power laws. Several such power laws will be mentioned further below.

The two types of fires mentioned add up to give the distributions typically seen in computer simulations, and explain the unconventional behavior of the forest fire model mentioned in the previous section. The left part of the fire size distribution of the forest fire model [see Fig. 2(b)] is mainly due to fires burning fractal percolation clusters, and the cutoff part is due to large compact fires. In contrast, in conventional critical systems the power-law part and the cutoff part are due to the same type of critical fluctuations. Since the two parts of the distribution become clearly separated only for very large ξ , as we will show below, the asymptotic exponent of the fire-size distribution is not visible in present-day computer simulations.

C. The scaling behavior

In the stationary state, the mean number of growing trees must equal the mean number of trees burning down, leading to [2]

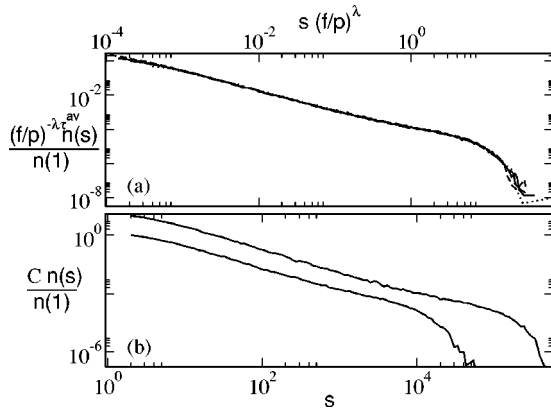


FIG. 2. (a) Superposition of the fire size distributions $n(s)$ of the SOC forest fire model for $L=1300$ and $f/p=0.000118$ (dashed line), 0.000169 (solid line), 0.00236 (solid line), and 0.000394 (dotted line). In order to make the curves collapse, the vertical axis had to be scaled with $(f/p)^{-\lambda_{av}}$, using the effective exponent $\tau^{av}=1.14$, which can be interpreted as an average exponent over a certain range of s values. (b) Fire size distributions $n(s)$ for $L=1300$ and $f/p=0.0001183$ (upper curve) and $f/p=0.001183$ (lower curve). The upper curve was shifted vertically by a factor $C=10$, in order to make the shapes of the two curves better visible.

$$\bar{s} = \frac{p(1-\rho)}{f\rho}. \quad (3)$$

\bar{s} diverges according to a power law in the limit $f/p \rightarrow 0$, implying that the size s_{\max} of the largest fires also diverges, and with it the correlation length ξ , which we define to be the radius of the largest fires. The cutoff fire size s_{\max} can be expected to scale as

$$s_{\max} \sim (f/p)^{-\lambda}, \quad (4)$$

with an exponent λ [3–5], which has a value close to 1.1. This leads to $\xi \sim (f/p)^{-\lambda/2}$ since the fractal dimension of the large fires is 2. (In contrast, earlier work was based on the assumption that large and small fires have the same fractal dimension, which was found to be $D \approx 1.96$ [5], with some authors not ruling out the value $D=2$ [4,3].)

Let s be the number of trees burnt during a fire, and $n(s)$ the size distribution of fires in the system, normalized such that $\int n(s) ds = \rho$. Since each tree is struck by lightning with the same probability, the size distribution of tree clusters is proportional to $n(s)/s$. We write

$$n(s) = n_1(s) + n_2(s), \quad (5)$$

with $n_1(s)$ being the contribution from the smaller, fractal fires, and $n_2(s)$ being the contribution from the compact fires that burn an entire patch. If there was no qualitative difference between the two types of fires, the scaling law, Eq. (1), would hold, from which one could derive the scaling relation

$$\lambda = \frac{1}{2-\tau}. \quad (6)$$

(This is obtained from the condition $\bar{s} = \int_1^\infty s n(s) ds / \rho$ and is given in many earlier publications.) However, since we have two different types of fires, we cannot expect this relation to hold. Figure 2(b) shows the size distribution of fires for different values of f/p . (The system size L was chosen large enough to avoid finite-size effects.) One can see in this figure that for s between 100 and 1000, $n(s)$ becomes steeper with decreasing f/p , while for smaller s values the two $n(s)$ curves coincide. (The reason that they are not on top of each other in the figure is that we have multiplied one of the curves by 10 for better visibility). Taking all available data together, one finds that for larger s , the value of f/p below which the asymptotic value of $n(s)$ (i.e., the value seen for $f/p \rightarrow 0$) becomes visible, is smaller. One can expect that the slope will grow beyond the values visible in the figure, and that only for sufficiently large s and sufficiently small f/p , its asymptotic limit value becomes visible. The steepest slope occurring in this figure has the absolute value $\tau=1.3$, which should be a lower bound to the asymptotic value of τ . [The value $\tau \approx 1.14$ given in many earlier publications was obtained by taking some average value along $n(s)$, which was less than its steepest slope.] A scaling collapse [see Fig. 2(a)] shows that the cutoff parts of the curves superimpose nicely, allowing us to derive a value $\lambda \approx 1.1$, which does not fit together with the scaling relation, Eq. (6). The same result for λ was obtained by Pastor-Satorras and Vespignani [19] using a moment analysis, confirming that the cutoff shows simple scaling behavior.

Next, let us discuss the properties of $n_1(s)$. As f/p decreases, the first part of $n(s)$ does not change any more. This indicates that $n_1(s)$ reaches an asymptotic form $n_1^*(s)$ as $f/p \rightarrow 0$, with a cutoff that depends on f/p . We therefore write

$$n_1(s) = n_1^*(s) \mathcal{C}_1(s/s_{\max, \text{fractal}}) = n_1^*(s) \mathcal{C}_1(s(f/p)^{\lambda_1}), \quad (7)$$

introducing the cutoff function $\mathcal{C}_1(s/s_{\max, \text{fractal}})$ for the distribution of the fractal fires and assuming that the maximum fractal fire size $s_{\max, \text{fractal}}$ scales with an exponent λ_1 . For sufficiently large s , $n_1^*(s)$ will reach an asymptotic power law with the “true” exponent τ . We can estimate the value of τ from the following argument: The large fractal fires stem from the percolation clusters in those patches that have a tree density close to the percolation threshold ρ_{perc} . Thus the probability density of finding a cluster of size s is proportional to the probability that ρ_{patch} of a large patch is large enough that percolation clusters of size s exist, multiplied by the probability density to find a cluster of size s in a system at the percolation threshold. The fire size distribution is proportional to s times the cluster distribution, as we mentioned above. The probability to find a cluster of size s in a percolation system is determined by the size distribution of percolation clusters:

$$n_{\text{perc}}(s) \approx s^{-\tau_{\text{perc}}} \mathcal{C}_{\text{perc}}(s/s_{\max, \text{perc}}) \quad (8)$$

with

$$s_{\max, \text{perc}} \propto (\rho_{\text{perc}} - \rho_{\text{patch}})^{-\sigma_{\text{perc}}} \quad (9)$$

and $\sigma_{\text{perc}}=91/36\approx 2.528$ and $\tau_{\text{perc}}=187/91\approx 2.055$ [18]. In these patches close to the percolation threshold, the tree density increases with time approximately as $\dot{\rho}_{\text{patch}}=p(1-\rho_{\text{perc}})$. Therefore, the probability that the density is within a distance $\rho_{\text{perc}}-\rho_{\text{patch}}$ of the percolation threshold is proportional to $\rho_{\text{perc}}-\rho_{\text{patch}}$, and the probability that a patch has tree clusters larger than s is proportional to $s^{-1/\sigma_{\text{perc}}}$ [see Eq. (9)]. The probability that a fire of size s occurs is consequently proportional to

$$s^{1-\tau_{\text{perc}}-1/\sigma_{\text{perc}}}\approx s^{-1.45}.$$

This means

$$\tau\approx 1.45.$$

Next, let us estimate the cutoff exponent λ_1 . As we have seen above, the radius ξ of the largest patches is proportional to $(f/p)^{-\lambda/2}$. The size of the largest fractal tree clusters is therefore proportional to $(f/p)^{-D_{\text{perc}}\lambda/2}$, with the fractal dimension D_{perc} of percolation clusters ≈ 1.56 , implying $\lambda_1\approx 0.86$. Beyond the cutoff size for fractal clusters, proportional to $(f/p)^{-\lambda_1}$, the size distribution of fires must be dominated by the compact fires and therefore by the size distribution of patches. Since $\lambda_1<\lambda$, the ‘‘bump’’ (which is dominated by the compact fires) should span a larger fraction of the fire size distribution for smaller f/p . Figure 2(b) shows that this is indeed the case.

Assuming that the patch size distribution $n_{\text{patch}}(s)$ scales, too, we suggest a scaling form

$$n_{\text{patch}}(s)\approx s_{\text{max}}^{b-2}s^{-b}\mathcal{C}_2(s/s_{\text{max}}), \quad (10)$$

with s being the number of sites in a patch, and $s_{\text{max}}\propto(f/p)^{-\lambda}$ being the area of the largest patch. Since most of the system is covered by large patches, b must be smaller than 2, requiring the factor s_{max}^{b-2} in Eq. (10) in order to normalize $\int sn_{\text{patch}}(s)ds$. The size distribution $n_2(s)$ for the compact clusters depends on $n_{\text{patch}}(s)$, but the relation between the two is nontrivial. The reason is the following: Assume that a patch is struck by lightning always when its density is so far above the percolation threshold that it burns down completely. In this case, the size distribution of the large fires would be proportional to s times the size distribution of the patches. However, in this case patches would never be destroyed. On the other hand, patches merge from time to time with neighbors, when the neighbor reaches a density above the percolation threshold before lightning strikes the patch with the higher density. In order to obtain a stationary patch size distribution, patches must therefore be destroyed from time to time. This can only happen if they are hit by lightning with a nonvanishing probability as long as their density is sufficiently close to the percolation threshold, such that smaller dense clusters of trees are left behind by the fire that can develop into small new patches. For this reason the size distribution of the large fires is different from s times the size distribution of patches. This will be seen also in the next section.

D. The exponent δ

Additional support for the picture that the fire size distribution is the sum of two qualitatively different contributions comes from the scaling behavior of the tree density. It has been known for a long time that the tree density approaches its critical value according to

$$(\rho_c-\rho)\sim(f/p)^{1/\delta},$$

with $1/\delta\approx 0.5$ [3–5]. (The most recent and probably most accurate value is 0.47 [19].) If the fire size distribution obeyed the scaling law, Eq. (1), one would expect δ to follow from

$$\rho_c-\rho=\int_{s_{\text{max}}}^{\infty}s^{-\tau}ds.$$

Assuming that conventional scaling [see Eq. (1)] holds and using Eqs. (4) and (6) this leads to

$$1/\delta=\frac{\tau-1}{2-\tau}.$$

With the apparent value of τ around 1.14, this would result in a value of $1/\delta$ much smaller than 0.47. With the asymptotic value $\tau=1.45$ (see below), $1/\delta$ would have to be much larger than 0.47. It has been pointed out recently that the observed value of δ makes corrections to simple scaling necessary [19], and a second contribution to $n(s)$ has been suggested, which has a larger exponent τ but the same cutoff as the main contribution, and which becomes negligible for sufficiently small f/p and sufficiently large s . In contrast to these authors, we argue that there occur not merely corrections to scaling, but that the scaling behavior of the SOC forest-fire model is fundamentally different from simple scaling. For this reason, there is no relation between the exponents δ and τ , since there is no single exponent τ describing the entire fire size distribution. Whether there exists another relation between δ and the fire size distributions n_1 and n_2 , we do not know.

III. SUPERPOSITION OF DIFFERENT TYPES OF FIRES

In order to show that the fire size distribution seen in simulations can indeed be the result of the superposition of the two mentioned types of fires, and in order to confirm that the asymptotic value of τ is 1.45, we superimposed the cluster size distributions of two-dimensional lattices that were homogeneously covered with trees, and that had tree densities between $\rho_{\text{after the fire}}=0.078$ and $\rho_{\text{max}}=0.625$, with weights derived from Eq. (2). This kind of superposition was suggested by Clar *et al.* in [16]. The values for $\rho_{\text{after the fire}}$ and ρ_{max} were measured, for instance, in [16]. But in addition to the superposition of the different tree densities we also superimposed different lattice sizes l , distributed according to Eq. (10) with $l=\sqrt{s}$ and cutoff $l_{\text{max}}=\xi=\sqrt{s_{\text{max}}}$. The lattices thus represent patches of different sizes and densities. In order to find the value of the exponent b , we performed superpositions for 20 different values of b from 0.1 to 2. The

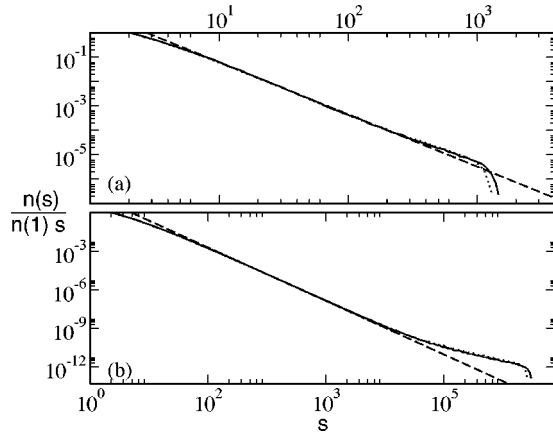


FIG. 3. (a) Size distribution of tree clusters $n(s)/sn(1)$ resulting from the superposition of lattices with $l_{\max}=50$ and $b=0.6$ (solid line: square lattice; dotted line: triangular lattice), and a power law with the exponent $\tau+1=2.14$ (dashed line). (b) The same for $l_{\max}=2000$ and $b=0.6$, compared to a power law with the exponent $\tau+1=2.45$. The tree densities we used cover the interval $[0.078, 0.625]$ for the square lattice and $[0.062, 0.534]$ for the triangular lattice.

results did not depend very much on b as long as b was smaller than 1, suggesting that the value of b is in the interval $(0,1)$, but not allowing us to fix it more precisely. The results are only reproducible when the statistics are sufficiently good. For this reason, we had to superimpose 10^4 or more systems.

The results are shown in Figs. 3(a) and 3(b). Please note that these figures give cluster size distributions $n(s)/s$ and not fire size distributions $n(s)$, i.e., the exponents are larger by 1. Figure 3(a) shows that the apparent exponent $\tau \approx 1.14$ typically found in simulations of the 2D forest fire model is reproduced by the superposition. The smaller slope for small s , and the bump followed by the cutoff, are reproduced as well. We have performed this superposition also for a triangular lattice. This lattice is most easily implemented by taking a square lattice and including next-nearest-neighbor couplings along one of the diagonals in each unit cell. As for the square lattice, the range of tree densities was obtained from simulations of the SOC model, and was found to cover the interval $[0.062, 0.534]$. One can see that the apparent exponent τ is the same as for the square lattice, explaining the “universality” of this exponent with respect to a change of the lattice type found earlier [5]. (All other figures shown in this paper are for the square lattice only.) Figure 3(b) shows that the distributions of the two cluster types separate for larger correlation length ξ , and that the slope of the part of the curve that stems from fractal clusters tends to $\tau=1.45$ as we calculated in Sec. II. A similar effect will be found in the coarse-grained model discussed in the next section [compare Fig. 5(a)].

Our results show also that the size distribution of the largest fires is related to the size distribution of patches in a nontrivial way, as mentioned in the previous section. If all large fires did burn complete patches, the bump of the fire size distribution would have a slope $-b+1$, which is positive. Since this is not the case, many tree clusters must be

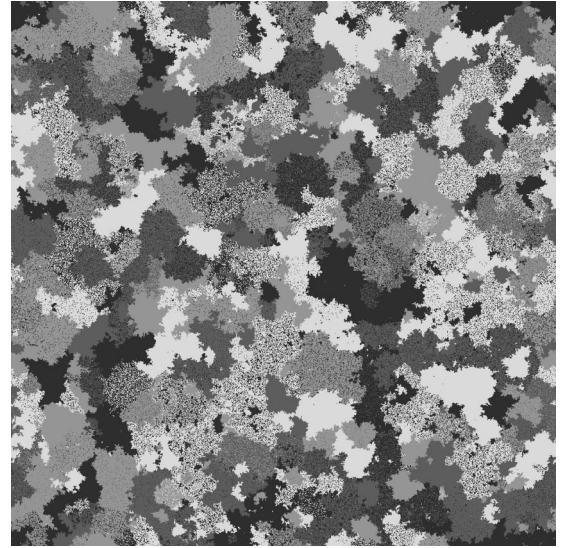


FIG. 4. Snapshot of the coarse-grained forest-fire model for $p=0.01$, $r=0.1$, $f=0.0001$, and $L=1000$. The tree density of a site is represented by its gray shade, with larger densities being darker.

contributing to $n(s)$ that are large but do not cover the entire patch. This consideration should hold for any value of s_{\max} . We expect, therefore, the value of ρ_{\max} to decrease slightly with increasing s_{\max} , such that there is always a nonvanishing contribution to $n(s)$ of clusters that are large but do not cover the entire patch.

We conclude that the superposition of homogeneous patches reproduces important features of the SOC FFM. It is also an efficient way of studying the regime of large correlation length, which is not accessible to direct computer simulations.

IV. A COARSE-GRAINED FOREST-FIRE MODEL

A. Definition of the model

In order to be able to study larger systems, we introduced a coarse-grained model where each site stands for a group of sites in the original model. The variable at each site of this coarse-grained model is the local tree density ρ_{site} , ranging continuously from 0 to 1. The rules of our coarse-grained model are the following: (i) the density at all sites increases per time step by a small amount $\Delta\rho_{\text{site}}=p(1-\rho_{\text{site}})$; (ii) Lightning strikes each site with a probability f . If the density of this site is below the percolation threshold $\rho_{\text{perc}}=0.59$, nothing happens. If the tree density on a site struck by lightning is above the percolation threshold ρ_{perc} , this site and the entire cluster of sites above the percolation threshold connected to it burn down. The density on a site after a fire is a random number between 0 and r . The parameter r takes short-range fluctuations in the density into account. The smaller r , the smaller the density fluctuations. Smaller r consequently means that the density at each site is the average of a larger number of sites in the original model. We therefore expect the coarse-grained model for small r to resemble the original FFM for large ξ .

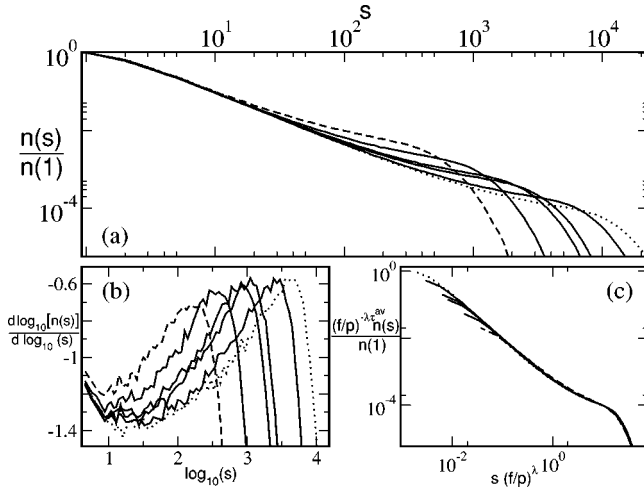


FIG. 5. (a) Fire size distribution $n(s)/n(1)$ of the coarse-grained forest-fire model for $f/p=0.0031$ (dotted curve), 0.005, 0.01, 0.0125, 0.025, and 0.05 (dashed curve), with the parameters $r=0.1$ and $L=1000$. (b) Slopes of the curves shown in (a). (c) Collapse of the fire size distributions of (a). In order to make the curves collapse, the vertical axis had to be scaled with $(f/p)^{-\lambda^{av}}$, using the effective exponent $\tau^{av}=1.25$, which can be interpreted as an average exponent over a certain range of s values.

B. Properties of the coarse-grained forest fire model

Although the coarse-grained model is not exactly the same as the original FFM, it shares many of its features. Figure 4 shows a snapshot of the coarse-grained model for $r=0.1$. The figure shows a patchy structure similar to the one in Fig. 1. In many patches one can see sites of two different densities. This indicates that lightning often strikes a patch before all of its sites (which cover a range of densities of the width r) have a local density above the percolation threshold, leaving behind some sites with a density just below the percolation threshold. If this happens several times within the same patch, one can expect the patch to be destroyed and replaced by a set of smaller patches. Such processes of birth and death of patches are not considered further in this paper, but of course they occur also in the original FFM, as can be seen in Fig. 1. As we have mentioned above, creation of new small patches must occur in order to balance merging and growth of patches in the stationary state.

Next, let us consider the size distribution of fires in the coarse-grained model. Figure 5(a) shows our simulation results for $r=0.1$ and different values of f/p . One can clearly see that the slope becomes steeper with decreasing f/p and appears to approach a limit slope. Figure 5(b) shows the slopes $d \log n(s)/d(\log s)$ as function of $\log(s)$, indicating that the predicted limit value 1.45 is indeed correct.

Figure 5(c) shows a collapse of the cutoff parts of the curves, giving $\lambda \approx 1.1$, just as in the original forest-fire model. We also performed a moment analysis of the fire-size distribution, giving the same result $\lambda \approx 1.1$.

Figure 6 shows the fire size distribution $n(s)$ for three different values of r , and for the same $f/p=0.01$. For smaller r , the slope becomes steeper and the cutoff bump becomes more pronounced, indicating that for smaller r the coarse-

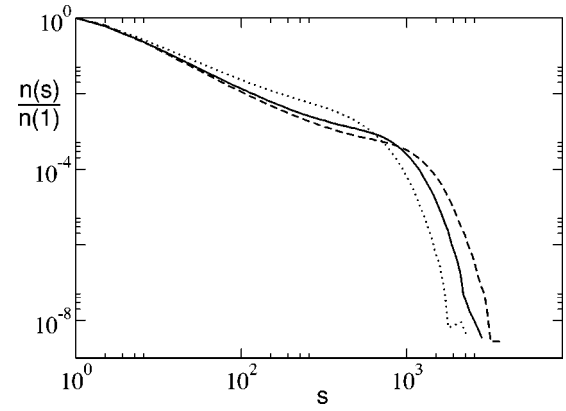


FIG. 6. Fire size distributions of the coarse grained model for $r=0.1$ (dashed curve), $r=0.2$ (solid curve), and $r=0.5$ (dotted curve). $L=1000$ and $f/p=0.01$ for all systems.

grained model resembles the original model on larger scales. For smaller r , the cutoff becomes larger. The reason is that for smaller r a site of the coarse-grained model corresponds to more sites of the original model. The same lightning probability f per site in the coarse-grained model corresponds to a smaller lightning probability in the original model when r is smaller.

Let us now estimate how many sites $z(r)$ of the original model correspond to a site in the coarse-grained model with parameter r . From Fig. 2(a) we find that

$$s_{\max} = A(f/p)^{-\lambda}$$

with $A \approx 30$. Similarly, we have for the coarse-grained model

$$s_{\max} = B(r)(f/p)^{-\lambda}.$$

From Fig. 5(c) we estimate $B(0.1) \approx 100$, and from the data shown in Fig. 6 we then obtain $B(0.2) \approx 66$ and $B(0.5) \approx 44$. Now, s_{\max} sites in the coarse-grained model correspond to $z(r)s_{\max}$ sites in the original model, and f in the coarse-grained model corresponds to a lightning probability $f/z(r)$ per site in the original model. Therefore we have

$$B(r)(f/p)^{-\lambda} = A(f/pz)^{-\lambda}/z,$$

leading to

$$z(r) = [B(r)/A]^{1/(\lambda-1)} \approx [B(r)/A]^{10},$$

resulting in $z(0.5) \approx 46$, $z(0.2) \approx 2650$, and $z(0.1) \approx 170000$. The length scales of the coarse-grained model are reduced by factors of the order 7, 50, and 400 for these three r values, compared to the original model.

A direct comparison of a fire size distribution of the original model and one of the coarse-grained model with $r=0.5$ confirms these findings. We searched for two fire size distributions such that the ratios of their f values and the ratios of their s_{\max} values are similar. This ratio turned out to be

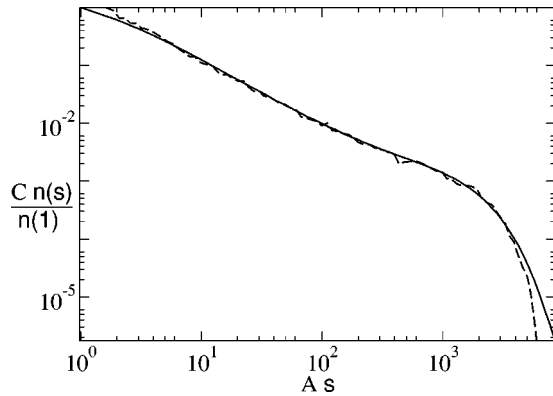


FIG. 7. Comparison of the fire distributions $n(s)$ obtained for the original SOC forest-fire model for $f=0.000\,001\,56$, $p=0.01$, and $L=800$ (dashed line, $C=41$, $A=1$), and for the coarse grained model for $r=0.5$, $f=0.000\,05$, $p=0.01$, and $L=1000$ (solid line, $C=1$, $A=44.9^{-1}$). The ratio between the two cutoffs, A , is the same as the inverse ratio between the two lightning probabilities f .

around 45, as shown in Fig. 7, and in agreement with the finding of the previous paragraph. Figure 7 shows also that the shapes of the two fire-size distributions, while similar, are not identical. Identical shapes cannot be expected, since the coarse-grained model is not completely identical to the original model on larger scales. For instance, inhomogeneities arising in the original model within an area of size $z(r)$ cannot occur in the coarse-grained model. This explains the difference in shape on small scales. On large scales, the difference in the shape of the cutoff is probably due to the fact that the process of slow destruction of large patches is slightly different in the two models. In both cases, lightning strokes hitting the patch when its density is only slightly above the percolation threshold make the patch more inhomogeneous. In the coarse-grained model, this leads to sites belonging to two widely different density intervals, as mentioned further above in the context of Fig. 4. In the original model, this leads to a couple of smaller dense tree clusters being left behind by the fire, as can be concluded from Fig. 1.

To conclude this section, our coarse-grained model, while not being exactly equivalent to the original model, shows the features expected of the original model on larger scales and confirms in particular the universality of the exponent λ and our conjecture that the exponent τ has an asymptotic value around 1.45. The detailed mechanism of birth and destruction of patches is somewhat different in the two models and leads to different shapes of the fire size distributions at small s and for the largest s .

V. DISCUSSION

In this paper, we have argued that the fire size distribution in the SOC FFM is the result of the superposition of two types of fires. The smaller ones are fractal percolation clusters, while the larger fires are compact and burn down a patch of a tree density above the percolation threshold. We supported this picture by a direct analysis of the model, by

the artificial superposition of the two types of fires, and by the introduction of a coarse-grained FFM.

One of our main results is that the asymptotic exponent for the fire size distribution is $\tau \approx 1.45$, and is visible only at length scales not accessible to present-day computer simulations. For values of the correlation length typically seen in computer simulations, the exponent τ has an apparent value that is smaller, and which seems to be insensitive to the lattice type used in the simulations. Furthermore, we found that the cutoff exponent λ has an universal value $\lambda \approx 1.1$, which is measured in the original FFM as well as in the coarse-grained FFM for different simulation parameters. The robustness of this exponent is additionally supported by our earlier finding that the correlation length shows nice scaling behavior in a generalized model where trees can be immune to fire [20].

We could not find the precise form of the size distribution of patches, although we presented evidence that it should be characterized by an exponent b smaller than 1. The patch size distribution is the result of a slow and highly nontrivial process of birth and merging and destruction of patches. This process also determines the size distribution of the large fires, for which we could not give an analytical expression.

In contrast to the exponent τ , we could not derive the value of the exponent λ from analytical arguments. We cannot rule out that its true value is $\lambda = 1$, and that there are logarithmic corrections that make it appear slightly larger than 1.

As we have shown, several scaling relations familiar from conventional critical systems and in particular from percolation theory do not hold in the SOC FFM. Instead, the FFM is a new type of nonequilibrium critical system that has no equivalent in equilibrium physics. It is characterized by different phenomena on different scales, and by a patchy structure indicating that neighboring sites tend to be synchronized by burning down during the same large fires.

By introducing the coarse-grained model, we have shown that there exists an entire class of models that share the same main features of a patchy structure and two qualitatively different types of fires, the asymptotic exponent $\tau \approx 1.45$, and the cutoff exponent $\lambda \approx 1.1$, while details such as the precise shape of the cutoff and the precise mechanism of birth and destruction of patches may differ.

We should point out that it is unclear whether the behavior in higher dimensions resembles that in two dimensions. Clearly, as long as the “patchy” structure with two qualitatively different types of fire occurs, the mean-field theory that neglects all spatial structure [21–23] cannot apply, and the system must be below its upper critical dimension.

Our results show that SOC can be caused by mechanisms fundamentally different from equilibrium critical phenomena. It remains to be seen to what extent different models are governed by different mechanisms. One clearly has to make a distinction between conservative models, such as the sandpile model, where energy can only be dissipated at the edges, and nonconservative models such as the forest-fire model. The unusual scaling behavior of the two-dimensional Abelian sandpile model is related to the multiple waves of topplings and is not observed in higher dimensions or other

sandpile models. In contrast, the SOC behavior of the forest-fire model seems to be closely related to the patchy structure, which implies a partial local synchronization. We expect that other nonconservative SOC systems are driven to criticality by mechanisms similar to the ones found in the FFM. This applies in particular to the SOC earthquake model [6], where a patchy structure with partial synchronization of neighboring sites was also found [24]. Very recently, it was additionally found that this model contains two qualitatively different types of avalanches: those within a “patch,” and those that enter it from outside and span the entire “patch” [25]. Other

related models, like a recently introduced threshold model [26], are yet too poorly investigated, but it can be expected that local synchronization and qualitatively different types of avalanches are also important in these systems.

ACKNOWLEDGMENTS

This work was supported by the Deutsche Forschungsgemeinschaft (DFG) under Contract No. Dr300-2/1, and by the EU under Contract No. ERPFMRXCT980183.

-
- [1] P. Bak, C. Tang, and K. Wiesenfeld, *Phys. Rev. Lett.* **59**, 381 (1987); *Phys. Rev. A* **38**, 364 (1988); P. Bak and M. Creutz, in *Fractals in Science*, edited by A. Bunde and S. Havlin (Springer, Berlin, 1994).
 - [2] B. Drossel and F. Schwabl, *Phys. Rev. Lett.* **69**, 1629 (1992).
 - [3] C. L. Henley, *Phys. Rev. Lett.* **71**, 2741 (1993).
 - [4] P. Grassberger, *J. Phys. A* **26**, 2081 (1993).
 - [5] S. Clar, B. Drossel, and F. Schwabl, *Phys. Rev. E* **50**, 1009 (1994).
 - [6] Z. Olami, H. J. S. Feder, and K. Christensen, *Phys. Rev. Lett.* **68**, 1244 (1992).
 - [7] P. Bak and K. Sneppen, *Phys. Rev. Lett.* **71**, 4083 (1993).
 - [8] M. Paczuski, S. Maslov, and P. Bak, *Phys. Rev. E* **53**, 414 (1996).
 - [9] H. J. Jensen, *Self-organized Criticality* (Cambridge University Press, Cambridge, UK, 1998).
 - [10] M. De Menech, A. L. Stella, and C. Tebaldi, *Phys. Rev. E* **58**, R2677 (1998).
 - [11] C. Tebaldi, M. De Menech, and A. L. Stella, *Phys. Rev. Lett.* **83**, 3952 (1999).
 - [12] B. Drossel, *Phys. Rev. E* **61**, R2168 (2000).
 - [13] S. Lise and M. Paczuski, *Phys. Rev. E* **63**, 036111 (2001).
 - [14] A. Honecker and I. Peschel, *Physica A* **239**, 509 (1997).
 - [15] S. Clar, B. Drossel, and F. Schwabl, *Phys. Rev. Lett.* **75**, 2722 (1995); S. Clar, K. Schenk, and F. Schwabl, *Phys. Rev. E* **55**, 2174 (1997).
 - [16] S. Clar, B. Drossel, K. Schenk, and F. Schwabl, *Phys. Rev. E* **56**, 2467 (1997).
 - [17] K. Schenk, B. Drossel, S. Clar, and F. Schwabl, *Eur. Phys. J. B* **15**, 177 (2000).
 - [18] D. Stauffer and A. Aharony, *Introduction to Percolation Theory* (Taylor & Francis, London, 1992).
 - [19] R. Pastor-Satorras and A. Vespignani, *Phys. Rev. E* **61**, 4854 (2000).
 - [20] B. Drossel, S. Clar, and F. Schwabl, *Phys. Rev. E* **50**, R2399 (1994).
 - [21] K. Christensen, H. Flyvbjerg, and Z. Olami, *Phys. Rev. Lett.* **71**, 2737 (1993).
 - [22] B. Drossel and F. Schwabl, *Physica A* **204**, 212 (1994).
 - [23] A. Vespignani and S. Zapperi, *Phys. Rev. E* **57**, 6345 (1998).
 - [24] A. A. Middleton and C. Tang, *Phys. Rev. Lett.* **74**, 742 (1995).
 - [25] S. Lise and M. Paczuski, *Phys. Rev. E* **64**, 046111 (2001).
 - [26] P. Sinha-Ray and H. J. Jensen *Phys. Rev. E* **62**, 3215 (2000).